AIP | Applied Physics Letters

Tuning the electrical properties of zirconium oxide thin films

Byeong-Ok Cho, Jianjun Wang, Lin Sha, and Jane P. Chang

Citation: Applied Physics Letters **80**, 1052 (2002); doi: 10.1063/1.1448667
View online: http://dx.doi.org/10.1063/1.1448667
View Table of Contents: http://scitation.aip.org/content/aip/journal/apl/80/6?ver=pdfcov
Published by the AIP Publishing

Tuning the electrical properties of zirconium oxide thin films

Byeong-Ok Cho, Jianjun Wang, Lin Sha, and Jane P. Chang[a)]
Department of Chemical Engineering, University of California, Los Angeles, California 90095

(Received 11 September 2001; accepted for publication 5 December 2001)

ZrO_2 films obtained using plasma-enhanced chemical-vapor deposition exhibit various electrical properties tuned by the flow rate ratio of O_2 to precursor-carrying Ar (O_2/Ar), which controls the hydrocarbon incorporation in the films and the interfacial layer formation. As-deposited ZrO_2 films obtained in oxygen-rich plasmas ($O_2/Ar \geqslant 1$) showed good electrical properties, including an overall dielectric constant of 16, a flatband voltage shift of -24 mV, an interfacial trap density of $\sim 10^{11}\ cm^{-2}\ eV^{-1}$, and a leakage current density of $3.3 \times 10^{-6}\ A/cm^2$ at an equivalent oxide thickness of 25 Å, suitable for metal–oxide–semiconductor device applications. © *2002 American Institute of Physics.* [DOI: 10.1063/1.1448667]

High-dielectric-constant materials are being actively researched to enable the continuous downscaling of ultra-large-scale integrated circuits, including their applications as a gate dielectric material in metal–oxide–semiconductor (MOS) transistors and as a storage capacitor in dynamic random access memory (DRAM) devices.[1] ZrO_2 has attracted much attention as one of the most promising candidates due to its high-dielectric constant of ~25, wide-band gap of 4.6–7.8 eV, low-leakage-current level, and superior thermal stability.[2–6] In DRAM applications, the dielectric films should be deposited over high-aspect-ratio capacitor structures, and chemical-vapor-deposition (CVD) processes with superior step coverage are preferred to physical-vapor-deposition processes. The plasma-enhanced CVD (PECVD) process has a distinct advantage over other thermal CVD methods in that higher deposition rates can be achieved at much lower substrate temperatures.[7] This low-temperature process can circumvent the diffusion of shallow junctions and reduce thermal strains leading to the defect generation.[8]

In this work, we deposited ZrO_2 films using zirconium tetra-tert-butoxide [$Zr(OC_4H_9)_4$, (ZTB)] as a metal–organic precursor, Ar as a carrier of the ZTB vapor, and O_2 as an oxidant in an electron-cyclotron-resonance (ECR) high-density-plasma reactor. The temperature of a bubbler containing liquid ZTB was controlled at 50 °C to provide a constant vapor pressure. The 2.45 GHz microwave power, the currents through upper and lower electromagnets, and the chamber pressure were set constant at 300 W, 120 A, 150 A, and 20 mTorr, respectively. We used 4 in. p-type Si(100) wafers with a resistivity of 1–2 Ω cm as the substrates, which were cleaned in a buffered HF solution for 30 s, rinsed in deionized water for 60 s, and dried in N_2 to yield a hydrogen-terminated surface. Neither heating nor biasing was applied to substrates during the PECVD experiments. The substrate temperature is expected to be slightly higher than room temperature, as Devine and Vallier[9] reported that the temperature of an unbiased and nonheated Si wafer rose to ~60 °C during depositing Ta_2O_5 using a PECVD process. No postdeposition annealing was performed in this work. The key parameter varied in this work was the O_2-to-Ar flow rate ratio (O_2/Ar), as it was determined to dominate the plasma gas composition and deposited film properties in our previous work.[10] A low O_2/Ar ratio resulted in high hydrocarbon content in the gas phase via decomposition of the bulky butoxyl ligands, while a high O_2/Ar ratio yielded an oxygen-rich plasma.

We measured the film thickness using a Gaertner L116B ellipsometer with a 632 nm He–Ne laser. All films were confirmed to be amorphous by the x-ray diffraction measurement. Capacitors were formed by sputter deposition of 300 nm Al on ZrO_2 followed by photolithographic patterning to form the top electrode with area sizes of 2×10^{-5}–8×10^{-5} cm^2. An Al contact was also made to the backside surface of the wafers. Capacitance–voltage ($C-V$) and current–voltage ($I-V$) characteristics were obtained using an HP 4284B LCR meter and an HP 4145B analyzer, respectively.

Figure 1 shows the $C-V$ curves normalized to the accumulation capacitance (C_{Acc}) at the electrode voltage of -4 V for capacitors built with thin ZrO_2 films deposited at different O_2/Ar ratios. The film thicknesses were 133 Å at

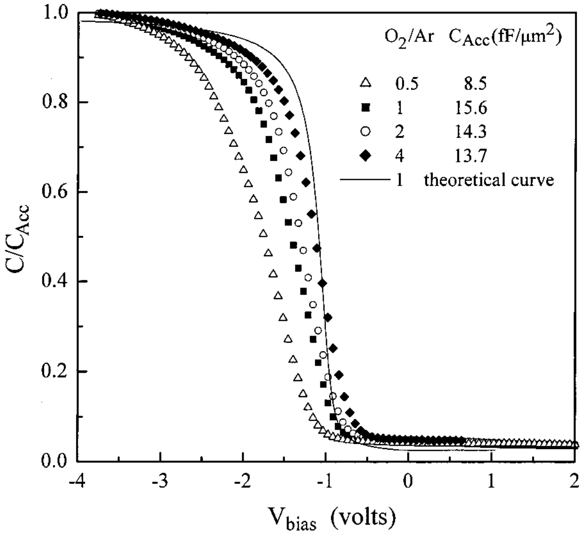

FIG. 1. Normalized $C-V$ curves of thin ZrO_2 films obtained at different O_2/Ar flow rate ratios. The solid line indicates the calculated curve according to the exact charge theory and a frequency of 1 MHz was used for the measurement.

[a)] Electronic mail: jpchang@ucla.edu

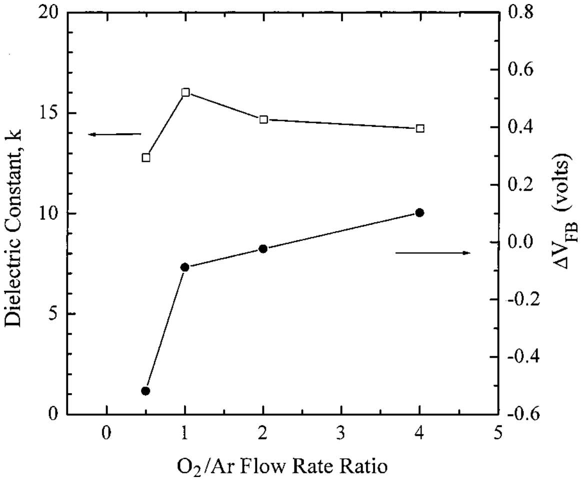

FIG. 2. Dependence of the dielectric constant and flatband voltage shift as a function of O_2/Ar flow rate ratios.

$(O_2/Ar)=0.5$ and 91 Å at $(O_2/Ar)=1$, 2, and 4. The theoretical $C-V$ curve shown for comparison with the experimental curve at $(O_2/Ar)=1$ was calculated from the exact charge theory[11] using the known oxide thickness of 91 Å, a dielectric constant of 16, and a dopant concentration of $8\times10^{15}\ \mathrm{cm}^{-3}$ in Si. The work function difference of -0.94 eV between the Al electrode and the p-type Si was also taken into account. Theoretical curves at other O_2/Ar ratios were almost identical to that at $(O_2/Ar)=1$ except for the different levels of C/C_{Acc} in the inversion regime $(C_{\mathrm{Inv}}/C_{\mathrm{Acc}})$. At $(O_2/Ar)=0.5$, where the plasma is hydrocarbon rich, the experimental and theoretical $C_{\mathrm{Inv}}/C_{\mathrm{Acc}}$ values differed only 5%. However, at $(O_2/Ar)\geqslant1$, where the plasma is oxygen rich, the experimental values of $C_{\mathrm{Inv}}/C_{\mathrm{Acc}}$ were always higher than the theoretical calculations by $\sim$70%. This indicates the presence of a lower-dielectric-constant interfacial layer between ZrO_2 and Si, decreasing the overall dielectric constant.[11,12]

To identify this interfacial layer, we analyzed the as-deposited films by high-resolution transmission electron microscopy (HRTEM). We confirmed the presence of an amorphous interfacial layer of $\sim$2 nm between ZrO_2 and Si. This layer could be either silicon oxide (SiO_x) (Refs. 13 and 14) or zirconium silicate $(ZrSi_xO_y)$ (Ref. 4) according to ZrO_2 deposition studies using similar process conditions in the literature. In either case, the diffusion of excess oxygen through ZrO_2 is necessary for interfacial layer formation.[4,13,14] We reported in our previous study[10] that oxygen became excessive at $O_2/Ar\geqslant1$ and its concentration increased with increasing O_2/Ar, which could lead to the formation of the observed interfacial layer. Moreover, taking into account the physical thicknesses of the interfacial layer and the ZrO_2 layer measured by HRTEM, and ZrO_2 dielectric constant ranging from 20 to 25,[3,15] we calculated a corresponding dielectric constant of the interfacial layer to be 5–7, which would explain the higher $C_{\mathrm{Inv}}/C_{\mathrm{Acc}}$ measurements discussed above.

The slopes of the $C-V$ curves gradually increase with the increasing (O_2/Ar) ratio, indicating the decrease in the interfacial trap density, D_{it}. We estimated the D_{it} to be $\sim10^{12}\ \mathrm{cm}^{-2}\ \mathrm{eV}^{-1}$ for films deposited at $(O_2/Ar)=0.5$ and $\sim10^{11}\ \mathrm{cm}^{-2}\ \mathrm{eV}^{-1}$ those at $(O_2/Ar)\geqslant1$ by Terman's method.[16] The decrease in D_{it} with increasing (O_2/Ar) is also likely resulting from the formation of a superior interface of either SiO_x or $ZrSi_xO_y$.[3]

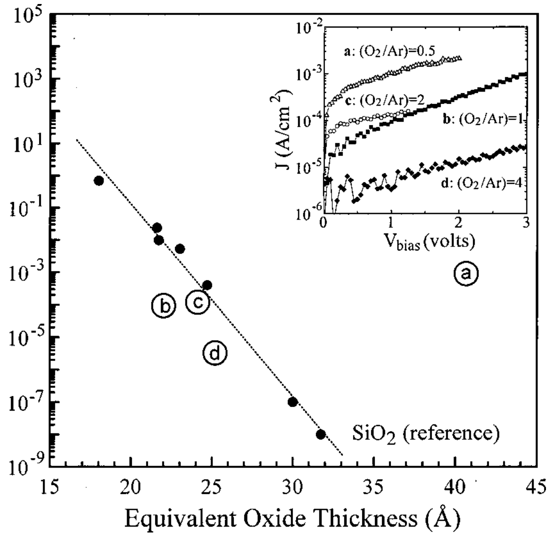

FIG. 3. Leakage current density as a function of equivalent oxide thickness. As-deposited ZrO_2 films at $(O_2/Ar)\geqslant1$ showed lower leakage levels than SiO_2 films of equivalent oxide thickness. Inset shows the leakage current density as a function of applied voltage.

Figure 2 shows that the dielectric constant of the deposited ZrO_2 increases from 13 at $(O_2/Ar)=0.5$ to 16 at $(O_2/Ar)=1$, then decreases gradually to 14 at $(O_2/Ar)=4$. The lowest dielectric constant at $(O_2/Ar)=0.5$ is related to the highest hydrocarbon content in the film.[17] We reported earlier[10] that a significant amount of hydrocarbon fragments from ZTB ligands can be incorporated into the ZrO_2 films under oxygen-deficient conditions, and a linear correlation was found between the x-ray photoelectron spectroscopy-determined carbon composition in ZrO_2 and the optical emission spectroscopy (OES) intensity ratio of C_2 (516.52 nm) to O (777.42 nm), which increases with decreasing (O_2/Ar). The compositional depth profile by Auger electron spectroscopy (AES) also showed the highest C/O atomic ratio in the film at $(O_2/Ar)=0.5$.

Figure 2 also shows the flatband (FB) voltage shifts, ΔV_{FB} $(=V_{\mathrm{FB}}-\phi_{MS})$, where V_{FB} is the flatband voltage and ϕ_{MS} is the Al–Si work-function difference. It is noteworthy that ΔV_{FB} scales linearly with increasing (O_2/Ar) at $O_2/Ar\geqslant1$. However, the thicker film deposited at $(O_2/Ar)=0.5$ shows a significant deviation $(-520\ \mathrm{mV})$. This indicates that the film deposited at $(O_2/Ar)=0.5$ is abundant in positive oxide-trapped charge (Q_{ox}) and fixed charge (Q_f), but the net charge decreases and eventually becomes negative as the (O_2/Ar) ratios increase. The density of fixed charges, Q_f/q, at $(O_2/Ar)=2$ is estimated to be at most $2.1\times10^{11}\ \mathrm{cm}^{-2}$, assuming the ΔV_{FB} contributed solely by Q_f.

The inset in Fig. 3 shows the leakage current density (J) versus bias voltage (V_b) characteristics from the PECVD films at different (O_2/Ar) ratios. The leakage current density at positive gate bias distinctly decreases with the increasing (O_2/Ar) ratio. The log(J) showed a linear dependence on $V_b^{1/2}$ at all O_2/Ar ratios, consistent with the Schottky emission mechanism,[18] where the charge conduction is dominated by the interface between ZrO_2 and Si substrate. As indicated by the $C-V$ and HRTEM analyses, the interfacial layer formation with increasing (O_2/Ar) ratios could dominate the decrease in J. The leakage current level under negative bias was much higher and invariant as (O_2/Ar) varied, indicating that the Al–ZrO_2 interface had a high level of defect density due to the sputter-deposited Al. Leakage current densities of the as-deposited PECVD ZrO_2 films measured at $V_b=1$ V are compared with those of SiO_2 in Fig. 3.[19] Although the film deposited at $(O_2/Ar)=0.5$ shows a much higher leakage level than SiO_2 at the same equivalent oxide thickness (EOT), the as-deposited films obtained at $(O_2/Ar)\geqslant 1$ yielded one to two orders of magnitude lower leakage current density than SiO_2. Especially the film at $(O_2/Ar)=4$ has a low-leakage-current density of $J=3.3\times 10^{-6}$ A/cm^2 at an EOT of 25 Å.

In conclusion, the electrical properties of a PECVD ZrO_2 film such as its dielectric constant, flatband voltage shifts, interfacial trap density, and leakage current density could be tuned by the O_2-to-Ar flow rate ratio, which controls the carbon content in the film and the formation of the interfacial layer.

The authors are grateful to Jae-Ho Min and Dr. Sang H. Moon at Seoul National University for the AES measurements and to Dr. Igor Levin at NIST for the HRTEM analysis. The authors acknowledge financial support from National Science Foundation Career Award No. CTS-9985511, a UCLA Chancellor's Faculty Career Development Award, and the donation of the ECR reactor from Bell Labs, Lucent Technologies.

[1] A. I. Kingon, J. P. Maria, and S. K. Streiffer, Nature (London) **406**, 1032 (2000).

[2] K. Sasaki and J. Maier, Solid State Ionics **134**, 303 (2000).

[3] G. D. Wilk, R. M. Wallace, and J. M. Anthony, J. Appl. Phys. **89**, 5243 (2001).

[4] W. Qi, R. Nieh, B. Lee, L. Kang, Y. Jeon, and J. C. Lee, Appl. Phys. Lett. **77**, 3269 (2000).

[5] P. Colpo, F. Ceccone, P. Sauvageot, M. Baker, and F. Rossi, J. Vac. Sci. Technol. A **18**, 1096 (2000).

[6] M. Cameron and S. M. George, Thin Solid Films **348**, 90 (1999).

[7] H. F. Frenck, E. Oesterschulze, R. Beckmann, W. Kulisch, and R. Kassing, Mater. Sci. Eng., A **139**, 394 (1991).

[8] E. Kim and S. Yoon, Thin Solid Films **227**, 7 (1993).

[9] R. A. B. Devine and L. Vallier, Appl. Phys. Lett. **68**, 1775 (1996).

[10] B. O. Cho, S. Lao, L. Sha, and J. P. Chang, J. Vac. Sci. Technol. A **19**, 2751 (2001).

[11] R. F. Pierret, *Field Effect Devices* (Addison-Wesley, New York, 1990), pp. 47–59.

[12] K. Lehovec, Solid-State Electron. **11**, 135 (1968).

[13] A. Kumar, D. Rajdev, and D. L. Douglass, J. Am. Chem. Soc. **55**, 439 (1972).

[14] L. Koltunski and R. A. B. Devine, Appl. Phys. Lett. **79**, 320 (2001).

[15] M. Houssa, V. V. Afana'ev, A. Stesmans, and M. M. Heyns, Appl. Phys. Lett. **77**, 1885 (2000).

[16] E. H. Nicolian and J. R. Brews, *MOS Physics and Technology* (Wiley, New York, 1982), pp. 325–328.

[17] L. M. Han, J. Pan, S. Chen, N. Balasubramanian, J. Shi, L. S. Wong, and P. D. Foo, J. Electrochem. Soc. **148**, F148 (2001).

[18] J. R. Yeargan and H. L. Taylor, J. Appl. Phys. **39**, 5600 (1968).

[19] S. C. Song, H. F. Luan, C. H. Lee, A. Y. Mao, S. J. Lee, J. Gelpev, S. Marcus, and D. L. Kwong, 1999 International Symposium on VLSI Technology, Systems, and Aplications. Proceeding of Technical Papers Catalog No. 99TH8453, 78 (1999).